

# Tidal accelerations and dynamical properties of 3-df pendula

René Verreault

Department of Fundamental Sciences  
University of Quebec at Chicoutimi  
555, Boul. de l'Université  
Saguenay (Quebec)  
Canada G7H 2B1  
[Rene\\_Verreault@uqac.ca](mailto:Rene_Verreault@uqac.ca)

## 1 Introduction

In the abundant literature on the spherical pendulum and in particular on the Foucault pendulum, the system generally considered consists of a point mass constrained to move on a spherical surface, when not projected on a horizontal plane. However if one is interested in studying very subtle perturbations of the spherical pendulum, it is necessary to deal with the "physical pendulum" altogether. An oscillating mass with 3-D extension usually lacks rotational symmetry about the spin axis, which is the line joining the instantaneous suspension point and the centre of mass, hereafter called the "bob", of the pendulum. The spin constitutes therefore an inherent third degree of freedom (df) for every physical pendulum. For the usual Foucault pendulum where a heavy mass is suspended by a metal wire, the third df takes the form of a torsion pendulum with a restoring torque originating from the elastic properties of the wire. However, for the ballborne pendulum of the Allais (paraconical) or Goodey type, [1][2] the spin motion is more complicated since there is essentially no restoring torque, except for a very small rolling friction torque at the area of contact. Spin motion is nevertheless ob-

served in practically every run, but to the author's knowledge, nobody, including Allais and Goodey, [1] has published on the subject. The experimental data suggest that there is a connection between the ellipticity of the bob orbit, the precession of the ellipse and the growth of an angle of spin. The purpose of this article is to study that relation and to try to find out whether, according to classical mechanics, it plays a role in the influence of the relative motion of the Earth, the Moon and the Sun on a 3-df pendulum.

## 2 Theory

In order to estimate the possible influence of the Moon, say, on the pendulum motion through tidal effects, one may first consider the main tidal components over a few days interval. On such a short arc compared to the whole Earth orbit, the motion of the Earth-Moon centre of mass is considered rectilinear enough to be the origin of an inertial system. However, the centre of the Earth is also moving at  $0,73$  Earth radius from that origin. If  $\Omega_M$  is the orbital angular velocity of the Moon, the centripetal acceleration of the Earth centre is  $0,73r\Omega_M^2$ , which, unlike the surface centripetal acceleration  $r\Omega^2$ , is neither constant nor included in the apparent gravitational acceleration  $\mathbf{g}$  at the Earth surface. The three orders of magnitude ratio between the two justifies taking the Earth centre coordinate system as inertial. The  $\Omega_M^2$  term could be added in a refined study if necessary.

As already pointed out by Munera, [3] the suspension point  $S$  is not a good laboratory reference for pendulum motion since, in a ballborne or paraconical pendulum for instance,  $S$  wanders somewhat erratically on a flat surface when the bob is moving. Even for a standard Foucault pendulum, the true height of the intersection point  $S$  between the vertical and the wire centre line changes with the amplitude and with the azimuth (suspension anisotropy) of the oscillation. This is namely responsible for the Kamerlingh-Onnes ellipses and precessions which are observed in practically every physical pendulum. [4] Therefore, experimental measurements are best made with reference to some alidade centre  $C$  which is fixed relative to the earth surface. Figure 1 shows the various vectors pertaining to that situation. The equation of motion in the laboratory system takes the form:

$$\ddot{\mathbf{r}}_4 = \ddot{\mathbf{r}}_2 - \frac{T\mathbf{r}_3}{mr_3} + \mathbf{g} + \sum_i (\mathbf{g}_i - \mathbf{g}_{iE}) - 2\boldsymbol{\Omega} \times (\dot{\mathbf{r}}_2 + \dot{\mathbf{r}}_3) \quad (1)$$

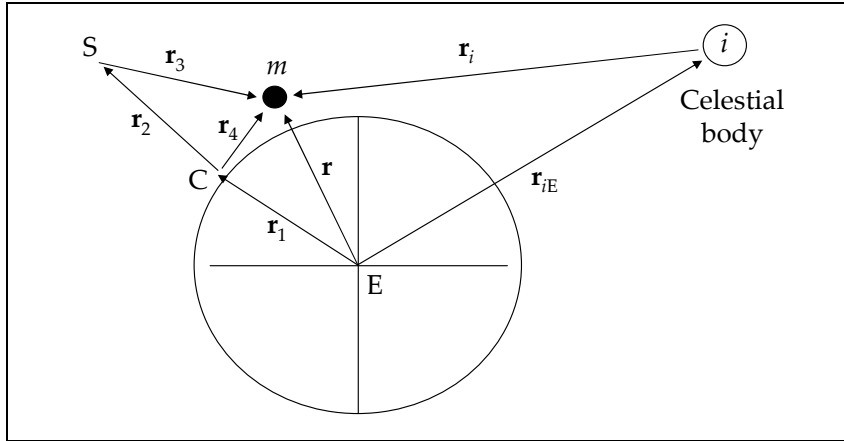


Figure 1. Pendulum geometry referred to the centre of the Earth.

Equation (1) is equivalent to Allais' Equation (4), p. 127 of his book, [5] except for a change of the laboratory origin in favor of the alidade centre C instead of the suspension point S.

It must be said at this point that the normal tidal effect due to the body  $i$  as the Earth rotates amounts to a periodical tilt of the local vertical at the  $i^{\text{th}}$  synodic rotation period of the Earth, eventually including some harmonics. For a 20-meter Foucault pendulum at mid latitudes, the centre of the elliptical bob orbits will describe its own ellipse with semi-axes of the order of 0,1 mm, under the influences of the Moon and the Sun. Such a tidal tilt would decenter a 1-meter pendulum by approximately 50  $\mu\text{m}$ .

### 3 Precession through gyroscopic effect

The airplane pilot's way of looking at gyroscopic effects is: if you want the horizontal axis of a rotating disk (propeller) to point upwards as per pushing on the bottom part of the disk plane, the effect will be as if the same push were applied 90° farther in the rotation direction. A cw rotating propeller as seen by the pilot will precess toward the right on a nose-up command, and vice-versa. This reasoning can be applied to the pendulum in each half-cycle as the Earth deviates the horizontally lying axis of swing at a steady rate.

Let us assume that a pendulum at the equator is swinging in a north-south vertical plane, after a start from the southern hemisphere at  $t = 0$ . The angular momentum vector about S is pointing eastwards for the first half-cycle. The Earth rotation is commanding "nose-down", so the pendulum will precess to the left. On the next half-cycle, the pendulum angular momentum is now point west and the Earth commands "nose-up". The result is a precession to the right exactly cancelling the effect of the preceding one. Hence the principal normal tidal effect due to the Moon and observable in the laboratory is:

- 1° from Section 2: an extremely small alternating tilt of the vertical with a 12,4-hour period and an amplitude of  $\sim 10^{-6}$  rad;
- 2° from above: absolutely no net precession due to that tilt.

#### 4 Precession and elliptical orbits due to perturbations at the pendulum frequency $\omega$

Perturbations having a rigid phase relation with the pendulum oscillation are especially prone to induce parametric amplification of some of the parameters. For instance, parametric amplification of the  $b$ -axis results in the growth of elliptical motion. Using perturbation methods, Pippard wrote an illuminating paper on that subject. [6] He considers, on the right-hand side of the differential equations, a perturbing force resolved into four components as follows (index  $c$  for cosine, and so on):

$$F_{ac} \cos \omega t + F_{as} \sin \omega t \quad \text{along the major axis,} \quad (2a)$$

$$F_{bc} \cos \omega t + F_{bs} \sin \omega t \quad \text{along the minor axis,} \quad (2b)$$

It turns out that the force component in phase with the motion on any axis generates elliptical motion, while a component at  $90^\circ$  out of phase with the motion on any axis generates precession. This is just a generalization of what happens with the Foucault precession, where the Coriolis force is at  $90^\circ$  out of phase with the motion along the major axis. More precisely, the precession angular velocity is given by

$$\Omega_p = (F_{bs} + \varepsilon F_{ac}) / 2ma\omega \quad (3)$$

where  $\varepsilon = b/a$ ; and the rate of growth of ellipticity is given by

$$\dot{\varepsilon} = -(F_{bc} - \varepsilon F_{as}) / 2ma\omega. \quad (4)$$

### 5 Lunar tidal effects on the pendulum

In Equation (1), the tidal term from the Moon is  $(\mathbf{g}_M - \mathbf{g}_{ME})$ . It is however pertinent to separate, as Allais did, the tidal contributions at various frequencies: first a rapidly varying term at the period of the pendulum  $T=2\pi/\omega$ , and second, a slowly varying term involving the Earth synodic period  $T_E \approx 24,8$  h and the Moon synodic period  $T_M \approx 29,5$  d. For that purpose, let us define an intermediate point C as the centre of the pendulum orbit, which coincides with the instantaneous rest point of the bob if the swing amplitude were zero. Refining Allais' formalism, one has

$$(\mathbf{g}_M - \mathbf{g}_{ME}) = (\mathbf{g}_M - \mathbf{g}_{MS}) + (\mathbf{g}_{MS} - \mathbf{g}_{ME}) \quad \text{(Allais)} \quad (5a)$$

$$\text{or } (\mathbf{g}_M - \mathbf{g}_{ME}) = (\mathbf{g}_M - \mathbf{g}_{MC}) + (\mathbf{g}_{MC} - \mathbf{g}_{MS}) + (\mathbf{g}_{MS} - \mathbf{g}_{ME}). \quad (5b)$$

Allais' last term above has already been dealt with in Section 3, at least for the Earth rotation period. It has been found that it results in tilting the vertical. So, added to any motion of the suspension S at frequencies well away from pendulum resonance, point C will describe a tiny ellipse, submillimeter in size, which could possibly be modulated at the longer lunar orbital period  $T_M$ . That tilting should be measurable. There remains now the short-period term, which can be interpreted with the help of Figure 2.

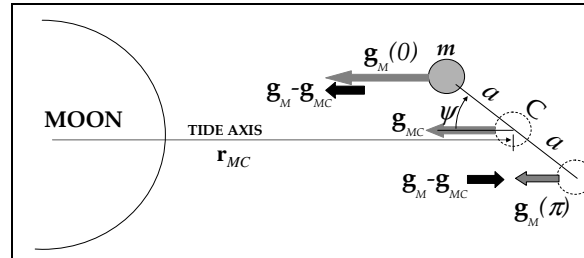


Figure 2. Tidal accelerations acting at the pendulum frequency (the vector modules have been exaggerated for clarity).

The main tidal accelerations experienced during the Earth rotation are indeed very slightly modified along the way by the fact that the pendulum oscillation superimposes the extremely small swing motion to the rapidly changing Moon-pendulum distance. Let the Moon-pendulum distance increase rapidly due to the Earth rotation entraining the laboratory away from the Moon and/or to the Moon orbit gaining altitude after its perigee.

The average acceleration  $\mathbf{g}_{MC}$  decreases in a "smooth" fashion while the instantaneous bob acceleration  $\mathbf{g}_M$  decreases more rapidly when the swing has a component away from the Moon and less rapidly when the swing is toward the Moon. This phenomenon amounts to another tidal contribution exactly in phase with the pendulum swing along each axis (cosine terms in Equation 2). It could be measured, if large enough, in the lab coordinates. Concerning the possibility of ellipse generation by the tidal tilting action, it is clear that the tilt tidal frequency is far too low to induce parametric amplification of  $b$  and, moreover, it is not commensurate with the pendulum period. So, the answer is no.

Allais has properly recognized those situations on page 127 of his book, [5] where he correctly neglects his term " $(grad_s U_i - grad_T U_i) = \text{déviation de la verticale}$ " [ $(\mathbf{g}_{MS} - \mathbf{g}_{ME})$ ] of Equation (5) above], which is now known to induce neither pendulum precession nor ellipse formation in the lab coordinates. He retains only his term " $(grad_G U_i - grad_s U_i)$ " [ $(\mathbf{g}_M - \mathbf{g}_{MS})$ ] of Equation (5) above].

Admittedly, he made an estimation of this term without considering the instantaneous rapid change in the Earth-Moon distance (from one to a few kilometers per pendulum period). The present author has addressed this problem in an unpublished paper. It turns out that for uniform and rectilinear relative Moon-pendulum motion, the result would be identical with the situation at rest, since over a finite number of swing periods, the average of the instantaneous positions of the bob and the average position of the ellipse centres coincide. On the other hand, at the extreme situations of relative acceleration, namely with the Moon near its perigee or apogee and with the laboratory at the latitude of a subsolar or sublunar eclipse point, the means of bob positions and ellipse centres no longer coincide. That non inertial tidal effect is at most of nearly the same magnitude of the linear one, mainly canceling it in the receding lab extreme or doubling it in the other extreme. To find out how the pendulum motion would be affected in the non accelerated case, let us assume the simpler situation of fixed Moon-pendulum distance and extremal lateral accelerations (polar experiment with equatorial eclipse).

From Equations (2) and Figure 2, one finds  $F_{as} = 0$  ;  $F_{bs} = 0$  ;

$$F_{ac}/m = (\mathbf{g}_{M \max} - \mathbf{g}_{MC}) \cos \psi \ ; \quad (6a)$$

$$F_{bc}/m = (\mathbf{g}_{M \max} - \mathbf{g}_{MC}) \sin \psi \ . \quad (6b)$$

Equation (3) states that there is no precession without the presence of an ellipse.  $F_{bc}$ , which is the tranverse component when the bob is at the end of the  $a$ -axis, generates an ellipse when there is none or amplifies an existing positive one. At the same bob position, the velocity along the  $b$ -axis is maximal if there is an existing ellipse and  $F_{ac}$  is tranverse to that velocity, which creates a precession of that ellipse.

Therefore, this submicroscopic tidal effect at the lab scale (or swing scale) will theoretically create no precession directly but the onset of an ellipse if there is none. Once there is an ellipse, a precession speed will grow up proportional to the  $b$ -axis.

For the other extreme situation of an equatorial experiment with Sun and Moon at zenith, there is no perturbing force in the orbit plane. Classical mechanics can only affect the period.

In short, Allais estimate is confirmed as to the magnitude of his tidal accelerations, namely as being 8 orders of magnitude below the values of  $F_{\mu\nu}/m$  that would account for the observations ( $\mu = a, b$ ;  $\nu = c, s$ ).

Of course, this last analysis may look very academical since this submicroscopic tidal effect originating from the Moon or any other celestial body can certainly not be measured by today's technology. But the situation may be different if large perturbing masses lie very close to the pendulum, like a concrete column or obese observers... In principle, an asymmetrical mass distribution around the pendulum leads to an anisotropy of the gravitational field potential well in which the pendulum evolves. For instance, suspension anisotropy can be analysed in terms of a very weak saddle-like field at point C, superimposed to the ideal spherical well. After all, Cavendish's torsional balance works on the principle of a saddle-like gravitational field. The question arises whether such a rotating saddle-like field originating from celestial bodies (space anisotropy) and from Earth rotation is sufficient to explain the tendency of the pendulum azimuth toward the low-energy axis. It seems that classical mechanics fails to answer the question so far.

## 6 The spin degree of freedom

In accelerated reference systems, nonlinear phenomena realize a coupling between otherwise independent df. The rigid body ballborne physical pendulum may be considered with 5 df, if the vertical motion of the suspension plane is neglected :

- 2 high-energy df of oscillation about the instantaneous suspension contact point,
- 1 medium-energy df of spin, with essentially no restoring torque, about a line through the moving contact point and the centre of mass,
- 2 low-energy df of horizontal translation of the average position, over a integer number of periods, of the contact point on the suspension plane.

On the other hand, one may find for the standard Foucault pendulum as many of 12 df:

- the 2 usual high-energy angular oscillation df about a slowly moving point in space;
- 4 medium-energy df : 1 spin with restoring torque about the wire centre-line; 2 transient orthogonal wobbling motions of the bob about the insertion point of the wire near its upper surface; 1 transient longitudinal wire vibration mode;
- 6 low-energy df: 1 long-term low-energy df being the pendulum length affected by temperature, and affecting the period; 3 long-term low-energy df of horizontal and vertical oscillation of the suspension point; 2 transient transversal vibration modes of the wire.

It is interesting to note that, once the initial bob wobbling and wire vibrations have died out, the bob-wire unit seems to act as a rigid body, at least for a time scale larger than the wobble natural frequency. The perturbing effect of the spin can be best visualized at the beginning of a swing cycle when the swing angular momentum is zero. Let us assume then that the pendulum has the spin velocity  $\vec{\dot{\varphi}}$ . Momentarily, the spin momentum constitutes by itself the total angular momentum of the pendulum.

In Figure 3a, the gravitational torque  $\mathbf{imgl}\theta_{\max} = d\mathbf{L}_\theta / dt$  tends to bring the vector  $\vec{\dot{\varphi}}$  parallel to the vertical axis. However, the Z-component of the angular momentum must stay constant. Indeed,  $\varphi$  and  $\psi$  do not appear explicitly in the Lagran-



gian for an isotropic pendulum with no spin restoring torque. For such *ignorable* variables, the vertical components of angular momentum constitute constants of the motion. [7] Even with a small restoring torque  $-D\phi$  or with suspension anisotropy being a very weak function of the azimuth  $\psi$ ,  $\dot{\phi}$  and  $\dot{\psi}$  are practically constant over one period.

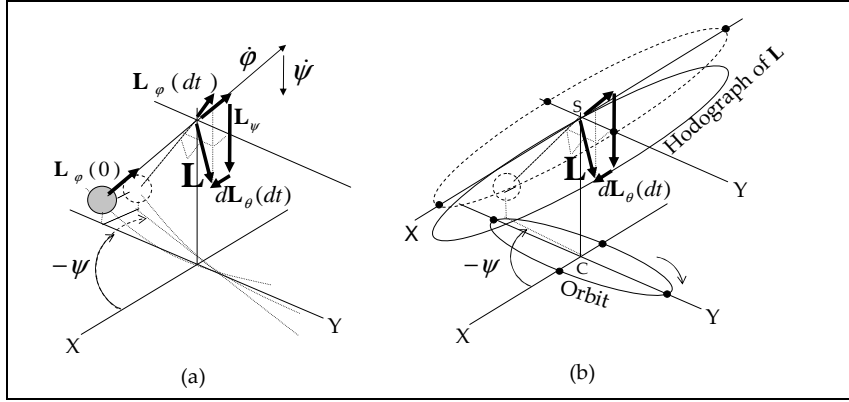


Figure 3. Perturbation originating from the spin. The horizontal scale has been exaggerated for clarity.

Consequently, the allowable motion at the start is in an horizontal plane instead of downwards as commanded by gravity. The support will therefore provide a reaction torque along the vertical axis corresponding to  $\mathbf{L}_\psi$  and  $\dot{\psi}$  in Figure 3a. The vertical momentum component associated with  $\dot{\psi}$  is

$$L_\psi = -L_\phi \cos \theta + L_{ab} ,$$

$L_{ab} = I_\psi \dot{\psi}_{ab}$  measures the vertical component of the orbital angular momentum associated with an elliptical orbit. It appears in Figure 3b as the height, in momentum units, of the hodograph of  $\mathbf{L}$  above (or below, as here) the suspension point S.

$$L_{ab} = \pm L(\theta) \sin \theta \approx \pm L(\theta_{\max}) \cdot \theta_{\max} = m\omega ab , \quad (\text{sign of } b).$$

The bob ,then, starts an horizontal motion towards the negative X, thus initiating an elliptical orbit. In the above example,

$$\dot{\epsilon} \cong -\dot{\phi} \frac{I_\phi}{I_\psi} = -\frac{2r^2}{5l^2\theta_{\max}^2} \dot{\phi} \approx -4 \cdot 10^{-4} \text{ s}^{-1} \quad (7)$$

In fact, the rather large value of  $\dot{\epsilon}$  takes the form of a short side-kick impulse at the beginning of the cycle, so that the ellipse remains at first quite narrow. For after a time  $dt$  of a few milliseconds, the increment  $d\mathbf{L}_\theta$  become larger than the spin momentum and overrides it, starting to bring the bob down. From then on, it is the spin that becomes the perturbing agent for the principal angular momentum  $\mathbf{L} = \mathbf{L}_\varphi + \mathbf{L}_\psi + \mathbf{L}_\theta$ .

Since  $\mathbf{L} = \mathbf{r}_3 \times \mathbf{v}$  must at all times be perpendicular to the radius vector  $\mathbf{r}_3$  and to the velocity  $\mathbf{v}$  of the bob along the right-handed orbit of Figure 3, it points slightly below the horizontal plane (dotted ellipse) containing the suspension point as the momentum origin. In practice,  $\theta_{\max}$  being small, the hodograph of  $\mathbf{L}$  lies very close to that plane. Moreover, the part of  $L_\psi$  which lies above the origin represents the perturbation due to the spin, namely a precession of the orbit at the rate

$$\dot{\psi}_p = -\dot{\phi} I_\varphi / I_\psi \quad \text{s}^{-1}. \quad (8)$$

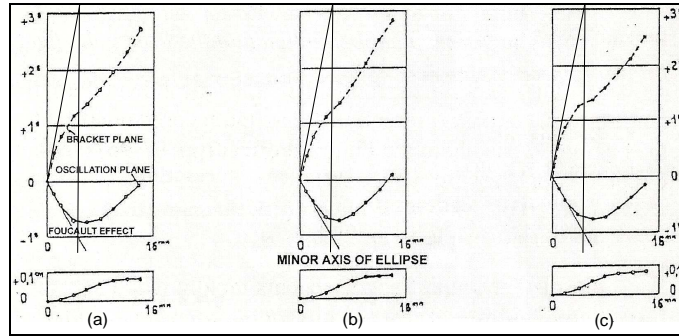


Figure 4. Monthly (a) and semi-monthly (b and c) averages of precession angles, spin angles and minor axis values within 14 min from start. The angle units are grads. The Foucault effect is  $\dot{\psi}_F = -2,94$  grads ( $-2,64^\circ$ ) per 14 minute run ( $-0,55 \cdot 10^{-4} \text{ s}^{-1}$ ). [8] Adapted from Allais' memoir to the NASA. [9]

## 7 A new interpretation of Allais' results

For the ballborne pendulum with no restoring torque, Equation (8) should be reversible, so that the onset of a precession should generate a corresponding spin. This can be seen in Al-

lais's Graph IV of its memoir for the NASA, [9] reproduced here in Figure 4. Allais' so-called "gyrostaticity coefficient"  $\gamma = I_\varphi / \bar{I}_\theta = I_\varphi \theta_{\max} / \bar{I}_\psi$ . So, at the start of Allais' experiment,  $I_\varphi / \bar{I}_\psi = \gamma / \theta_{\max} = 0,325$ , making the slope of the spin angle ("bracket plane" in Figure 4) 3,08 times steeper than the negative of the Foucault slope. The tangent lines added on Figure 4 illustrate the very good agreement with the above theory.

When spin kinetic energy or minor axis kinetic energy are growing, the energy must come either from a separate excitation or from a coupling between degrees of freedom. Combining Equations (7) and (8), one has

$$\dot{\phi} = c_{\varphi\psi} \dot{\psi}_p + c_{\varphi\varepsilon} \dot{\varepsilon} \quad (9)$$

From Equations (7) and (8),  $c_{\varphi\psi} = c_{\varphi\varepsilon} = -3,08$ .

Representing as in Figure 3b the momentum space with an origin at S, it can be seen that the precession and ellipse growing contributions from the spin are separated by the origin level: ccw precession and ccw elliptical increments belong to the positive (above S) half of momentum space, and vice-versa. The coupling involved in Equation (9) obviously comes from the motion constraint that the vertical component of angular momentum must remain constant if  $\varphi$  and  $\psi$  are ignorable variables. Although the Airy precession speed, [10] not shown in Figure 3, is usually too small to be illustrated for a long Foucault pendulum, it is far from negligible in Allais' paraconical pendulum, where  $l^2$  is  $O(1)$  m<sup>2</sup>. Equation (9) should then be re-written:

$$\dot{\phi} = c_{\varphi\psi} (\dot{\psi}_F + \dot{\psi}_A) + c_{\varphi\varepsilon} \dot{\varepsilon} , \quad (10)$$

$$\text{with } \dot{\psi}_A = (3/8)\omega ab / l^2 . \quad (11)$$

It is interesting to note that, in accordance with Equation (10) where  $c_{\varphi\varepsilon} < 0$ , the maximum growth rate of minor axis coincides with a minimal slope of the spin curve in Figure 4.

Allais' data on swing amplitude are not precise enough to enable an assessment of energy transfer from that df to the other ones. However, it is found that the only precession contribution other than Foucault precession (circular anisotropy characterized by non degenerate circular eigenmodes) is Airy precession, [11]

and that the external influence from any source takes the form of linear (suspension or space) anisotropy characterized by non degenerate linear eigenmodes with different periods for swing directions at  $90^\circ$  from one another. Allais states indeed in his equations, [11] that the precession angles that he observes outside the Foucault effect are solely explained by the Airy effect on the ellipses generated from suspension and/or space anisotropy.

However, from the minor axis value of Figure 4 after 14 minutes ( $\dot{\epsilon} = 0$ ), Equation (11) gives  $\dot{\psi}_A = 1,1 \cdot 10^{-4} \text{ s}^{-1} = -2,0 \dot{\psi}_F$ , giving, after 14 min, 5,4 grads of Airy precession. But from the experimental slope of the precession angles at that time,  $\dot{\psi}_{\text{exp}} \approx -0,5 \dot{\psi}_F$ , allowing for other precession contributions.

Roughly 4 grads of Airy effect are missing.

There should also be an "Airy-like" contribution arising from the asymmetry of the ellipsoid of inertia, whose axes stay within a few degrees of the swing azimuth. From Allais' asymmetry data, [12] the disk-shaped vertical bob lies indeed in a plane close to the major-axis azimuth. The resulting longer swing period in the major axis direction should then enhance the Airy effect, contrary to what is observed in Figure 4. The missing positive Airy-like precession speed that is due to anisotropy axes which are somewhat bound to the swing azimuth, is obviously transferred to a negative spin contribution 3 times as large which is subtracted from the Foucault-induced spin (9,0 grads after 14 min). The missing 6,3 spin grads can therefore account for +2,15 grads of precession, which is rather close to the missing 2,5 grads of Airy effect alone. Allais seems to affect space anisotropy solely to changes in minor axis. There might also be a direct precession effect which does not explicitly show up in building ellipses, and which may be masked by the buffering behavior of the spin df. That would be consistent with eclipse effects on torsion pendula. [13] [14]

## 8 Spin characteristics of the Foucault pendulum

Because of the spin restoring torque of the Foucault pendulum, a steady spin-inducing perturbation cannot build up spin angle indefinitely. Its action in a given direction is limited to a fraction of the spin period. Hence, the coupling constants between spin angle, minor axis swing amplitude and precession

angle must be much smaller than with the short and rigid ball-borne pendulum. Thanks though to the high precision video recording of pendulum motion achieved in the 2001 Chicoutimi experiment, [15] the first evidence of spin-orbit coupling with a long Foucault pendulum has been demonstrated by the author. The observations involve the simultaneous imaging of an array of luminous spots on an alidade fixed to the laboratory floor at the same height as the bob top surface, and a similar array of luminous spots attached to the top surface of the bob itself. Strictly speaking, this system records the relative motion of the insertion point of the flexible wire into the bob top surface. Through the use of deflecting mirrors, the camera, no matter its size, has a bird's view from a point  $\sim 2$  cm beside the suspension point, thus measuring essentially parallax free angles from the vertical. In practice, once the initial wobbling and string modes have died out, it is assumed that the motion of the centre of mass is recorded. Moreover, since the deflecting mirror is solidary with the suspension rig, suspension motion appears as a relative alidade motion in the image. In the 2009 Gifu experiment (Japan), alidade pseudo-oscillations in phase with the pendulum could demonstrate suspension-beam flexion and torsion as small as  $10^{-7}$  rad for a swing amplitude of 0,015 rad. That ended up in measurable pendulum anisotropy in the form of orthogonal swing periods differing by 3 parts in  $10^{-5}$ . Similarly, in the above mentioned 12-hour Chicoutimi experiment, the direct lunisolar tide effect could at most be seen as a complete conical sweep of the vertical along a 0,4 mm-radius circle on the floor. [15] Comparing it with the expected value in Section 2, this may include a small strain of the hosting cathedral as the Sun shines around the stone walls.

That particular experiment was started with a one-turn spin angle in order to see eventual interactions between spin and precession. In aftermath, the author argues that the Longden corked wire anisotropy can be eliminated this way, [16] since the eventual anisotropy axes actually swept an angle range between  $\pi$  and  $\pi/2$  for the totality of the experiment (spin time constant = 16 h).

Incidentally, beside spin-orbit coupling and a Foucault effect of  $\Omega_F = -11,25$  °/h , the precession angle of that 17,4 m long pendulum showed oscillations components in phase with the 3 most important harmonics of the tide in the nearby Saguenay River, albeit with different amplitude ratios (as Allais also found

out). Needless to say, both the direct lunisolar influence and the gravitational influence of the alternating water mass in the river fall short of explaining the measured accelerations by 8 and 4 orders of magnitude respectively. The data fit the precession equation below to  $\pm 15\%$ , except for the last spin-orbit term:  $\pm 30\%$ . N.B.: The precession speed oscillation due to the  $360^\circ$  spin had a non negligible amplitude :  $\dot{\psi}_{\phi_{\max}} = \omega_{\phi} A_{\phi} = 2,7 \text{ } ^\circ/\text{h} !$

$$\begin{aligned} \psi = & \Omega_F t + A_1 \cos(\omega_{T_1} t + \delta_1) \\ & + A_2 \cos(\omega_{T_2} t + \delta_2) + A_6 \cos(\omega_{T_6} t + \delta_6) \\ & + A_{\psi} \cos(2\Omega_F t + \delta_{\psi}) + A_{\phi} \cos(\omega_{\phi} t + \delta_{\phi}); \end{aligned} \quad A_{\psi} : \text{anisotropy term}$$

$$\begin{aligned} \psi = & [-360^\circ/32 \text{ h}]t + 1,68^\circ \cos[(2\pi t/24,8 \text{ h}) + 2,2] \\ & + 1,05^\circ \cos[(2\pi t/12,4 \text{ h}) + \delta_1 + \pi] + 0,38^\circ \cos[(2\pi t/4,1 \text{ h}) + \delta_1 - \pi/2] \\ & + 0,35^\circ \cos[(2\pi t/16 \text{ h}) + 4,9] + 0,03^\circ \cos[(2\pi t/212 \text{ s}) + \pi/2] \end{aligned}$$

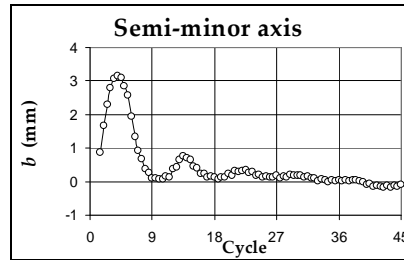


Figure 5. Effect of an initial spin on a 7,2-meter long Foucault pendulum in Tahiti. The bob design allowed for rapid spin damping over a few swing cycles.

A recent experiment in Tahiti (2010) is now in preliminary processing using a new proprietary pendulum analysis software. Different parameters are obtained at every half cycle with a precision unattained before. That experiment could be run with no spin by feeding the wire through the bob in a fixed capillary and then clamping it underneath. The wire torsion was hindered by friction inside of the capillary. Figure 5 shows the correspondence between minor axis and precession speed after an undesired  $10^\circ$  initial spin. The 7,2-meter pendulum had a spin period of 8,5 swing periods. A +3-mm  $b$ -axis yields a ccw precession speed increment of  $0,8 \text{ } ^\circ/\text{h}$ , which fades out within  $\sim 30$  swing cycles. It reaches up to 20% of the ccw,  $4,53 \text{ } ^\circ/\text{h}$ , Foucault effect in Papeete.

## 9 Conclusion

It can be seen from the above that the spin  $df$  plays an essential role in the short ballborne pendulum. It may yield a buffering action that will mask eventual direct precession contributions arising from an external pendulum perturbation. In that sense, Allais might have erroneously reserved exclusively minor axis changes to all the external influences, explaining his precession observations merely by the subsequent Airy effect. The long Foucault pendula show unexplained precession contributions orders of magnitude larger than the practically negligible Airy precession. Direct precession reveals the existence of circular anisotropy in the surrounding field, which appears consistent with many observations on torsion pendula.

The author acknowledges a significant instrumental facilitation of this fundamental research by Rio Tinto Alcan.

## References

- [1] T.J. Goodey, *private communication* (Gifu, Japan, 2009).
- [2] M. Allais, *L'Anisotropie de l'Espace* (Paris: Clément Juglar, 1997), p. 81.
- [3] H.A. Munera, *private communication* (Maldivian Islands, 2010).
- [4] K. Kamerlingh Onnes, *Nieuwe Bewijzen voor de Aswenteling der Aarde*, Thesis, Rijksuniversiteit te Groningen, Groningen, NL, 1879, 290 p.
- [5] M. Allais, *op. cit.*, p. 127.
- [6] A.B. Pippard, *The parametrically maintained Foucault pendulum and its perturbations*, Proc. R. Soc. London **A420**, 1988, p. 81-91.
- [7] D.A. Wells, *Lagrangian dynamics* (New York: Schaum, 1967), p. 235.
- [8] M. Allais, *L'Anisotropie de l'Espace* (Paris: Clément Juglar, 1997), p. 93.
- [9] M. Allais, *The "Allais Effect" and my Experiments with the Paraconical Pendulum 1954-1960*, a memoir prepared for NASA, 1999, available online at: <http://www.allais.info/alltrans/nasarep.htm>
- [10] G.B. Airy. *On the Vibration of a Free Pendulum in an Oval differing little from a Straith Line*, Proc. Royal Astron. Soc., 1851, Vol. XX, p. 121-130.
- [11] M. Allais, *op. cit.*, p. 120-122.
- [12] M. Allais, *op. cit.*, p. 85.
- [13] E. Saxl and M. Allen, *1970 solar eclipse as "seen" by a torsion pendulum*, Phys. Rev. D, 1971, vol. 3, no. 4, p. 823-825.
- [14] T.J. Goodey, A.F. Pugach and D. Olenici, *Correlated anomalous effects observed during a solar eclipse*, J. Adv. Res. in Physics, 2010, vol. 1, no. 2, 8p.
- [15] R. Verreault et S. Lamontagne, *Téledétection aérospatiale et Pendule de Foucault*, Revue Téledétection, 2007, vol. 7, n° 1-2-3-4, p. 507-524.
- [16] A.C. Longden, *On the irregularities of motion of the Foucault pendulum*, Phys. Rev., 1919. Vol. XIII, p. 251-258.